What caused the increase of tropical cyclones in the western North Pacific during the period of 2011–2020?

Haili Wang[1,2,3] · Chunzai Wang[1,2,3]

Abstract

Based on satellite data after 1979, we find that the tropical cyclone (TC) variations in the Western North Pacific (WNP) can be divided into three-periods: a high-frequency period from 1979 to 1997 (P1), a low-frequency period from 1998 to 2010 (P2), and a high-frequency period from 2011 to 2020 (P3). Previous studies have focused on WNP TC activity during P1 and P2. Here we use observational data to study the WNP TC variation and its possible mechanisms during P3. Compared with P2, more TCs during P3 are due to the large-scale atmospheric favorable conditions of vertical velocity, relative vorticity and relative humidity. Warm sea surface temperature (SST) anomalies are found during P3 and migrate from east to west, which is also favorable for TC genesis. The correlation between the WNP TC frequency and SST shows a significant positive correlation around the equator and a significant negative correlation around 36°N, which is similar to the warm phase of the Pacific Decadal Oscillation (PDO). The correlation coefficient between the PDO and TC frequency is 0.71, above the 95% confidence level. The results indicate that the increase of the WNP TC frequency during 2011–2020 is associated with the PDO and warm SST anomalies.

Keywords Tropical cyclone · Western North Pacific · Pacific Decadal Oscillation

1 Introduction

Tropical cyclone (TC) is one of the most intense weather systems in the world. A TC is called a typhoon when its wind speed exceeds 34 knots in the Western North Pacific (WNP). The WNP basin (0º-30ºN, 100ºE-180º) exhibits a high level of TC activity and is the most active region globally. About 26 named TCs occurred over the WNP basin each year on a climatological average, leading to huge loss of life and property (Zhang et al., 2009, Wang et al., 2021). Many studies point out an increasing pattern of TC-induced damages over

the past several decades (Knutson et al., 2010; Mendelsohn et al., 2012; Peduzzi et al., 2012). A better understanding of how the behavior of TCs may change (such as their frequency) has scientific and socio-economic value. Under the background of global warming, whether the number of TCs is increasing has attracted much attention.

Great efforts have been put in improving our understanding of changes in TC activity (Yang et al. 2018; Zhang et al. 2018b; Liu et al., 2019; Zhao and Wang, 2019; Yamaguchi et al., 2020). Numerous studies have shown the favorable large-scale conditions for TC formation (Bister and Emanuel, 1997; Ritchie and Holland, 1997; Molinari et al., 2000; Nolan et al., 2007; Vu et al., 2020; Walsh et al., 2020). Several conducive conditions are: (a) warm sea surface temperature (SST); (b) weak vertical wind shear; (c) high relative humidity; and (d) large vorticity. Understanding the environmental conditions that cause changes in TC genesis is very important for practical applications (such as TC forecasting).

TCs show significant variability at multiple time scales, due to variations in climate forcing (Wang and Chan 2002; Vecchi and Soden 2007; Kim et al. 2008; Zhan et al. 2012; Li and Zhou 2013; Lin and Chan 2015; Wang et al. 2015;

✉ Dr. Chunzai Wang
  cwang@scsio.ac.cn

1   State Key Laboratory of Tropical Oceanography, South
    China Sea Institute of Oceanology, Chinese Academy of
    Sciences, 510301 Guangzhou, China

2   Southern Marine Science and Engineering Guangdong
    Laboratory (Guangzhou), 511458 Guangzhou, China

3   Innovation Academy of South China Sea Ecology and
    Environmental Engineering, Chinese Academy of Sciences,
    510000 Guangzhou, China

Mei and Xie 2016). The Madden–Julian Oscillation (MJO) with a 30–90 day period can regulate WNP TC activity (Li and Zhou, 2013; Liu et al., 2021; Wang et al., 2018; Zhao and Wang, 2019). In the WNP basin, the active phase of the MJO enhances the local convection, which in turn leads to the increase in TC activity in the basin. The quasi-biweekly oscillation is another intra-seasonal mode, but with a more localized effect, that also affects WNP TC activity (Li and Zhou 2013). The El Niño-Southern Oscillation (ENSO) is known as the main phenomenon occurring at interannual time scales (Trenberth and Caron 2000; Timmermann et al. 2018; Kim et al. 2020). ENSO has significant impacts on WNP TCs (Kim et al., 2011). Zhao and Wang (2016, 2019) examine a stronger interannual relationship between ENSO and TCs in the WNP during the boreal summer from 1998 to 2015. The correlation is 0.60 at the 95% confidence level. At decadal time scales, many factors affecting the TC frequency have already been suggested. Researchers mainly focus on the following factors: (a) the strengthened western North Pacific subtropical high (Liu and Chan, 2020); (b) the anomalous westward WNP SST gradient (Choi et al., 2015); (c) phase shifts of the Pacific Decadal oscillation (PDO) (Zhao and Wang, 2016); (d) the interdecadal Pacific oscillation (He et al., 2015; Zhao et al., 2018), and also (e) the Atlantic Multi-decadal Oscillation (AMO) (Zhang et al., 2020; Zhang et al., 2017).

Most studies suggest that the frequency of WNP TCs decreased from 1979 to 2010 (Tu et al., 2009; Yokoi and Takayabu, 2013; Hsu et al., 2014). Few studies have examined the change of TC activity from 2010 to 2020. Most of the previous analyses on TCs focus on the first or the second half of the year, or a certain period of the year, and the number of TCs throughout the year is less covered in previous studies. With global warming and the emergence of various extreme weather phenomena, how did the TC frequency per year change during 2011–2020 compared to the pre-2010 decades? What caused those changes? To our knowledge, these issues have not been explained in previous studies. Here we investigate the possible reasons associated with the changes in the WNP TC frequency during 2011–2020 based on observations and reanalysis data.

The aim of this paper is to explore the change of the WNP TC frequency, and the corresponding local large-scale atmospheric changes and remote oceanic SST changes. The rest of this paper is organized as follows. Section 2 describes the data and method used in this study. The TC increase is illustrated in Sect. 3. In Sect. 4, we explore the possible influences of large-scale atmospheric environment and oceanic conditions associated with TC increase. The discussion and conclusions are presented in Sect. 5.

2 Data and method

2.1 TC data

The TC best-track data, including the TC intensity, latitude and longitude, are from the United States Joint Typhoon Warning Center (JTWC). The selected period for the present study is the period after the beginning of the satellite era from 1979 to 2020 (https://www.ncdc.noaa.gov/ibtracs/index.php?name=ib-v4-access). In this study, we focus on the TC frequency throughout the year (from January to December). The TC frequency in this study is calculated over the whole WNP region. The WNP domain (0°–30°N, 100°E–180°) is divided into 5° × 5° resolution grid boxes. TC genesis positions are counted for each grid box. The first position of a TC recorded in JTWC is defined as the TC genesis location. Student's t test is performed to test statistical significance.

2.2 Atmospheric and SST data

The monthly mean atmospheric fields (e.g., winds) are obtained from the United States National Centers for Environmental Prediction and National Center for Atmospheric Research (NCEP/NCAR) II monthly reanalysis dataset with a 2.5° × 2.5° grid (Kalnay et al. 1996) (https://psl.noaa.gov/data/gridded/). The monthly mean SST is taken from the United States National Oceanic and Atmospheric Administration (NOAA) Extended Reconstruction SST version 5 (ERSSTv5) with a resolution of 2° × 2° (Huang et al. 2017).

2.3 Selection of ENSO events

The Niño 3.4 SST index is calculated from the HadISST1 dataset (Rayner et al. 2003) (https://psl.noaa.gov/gcos_wgsp/Timeseries/Nino34/). The Oceanic Niño Index (ONI) from the Climate Prediction Center is used to distinguish El Niño and La Niña years based on a 0.5 °C threshold. (https://origin.cpc.ncep.noaa.gov/products/analysis_monitoring). The years with SST anomalies more positive (more negative) than 0.5 °C (−0.5 °C) during October to December are defined as El Niño (La Niña) years. The other years are considered as neutral years. Detailed classifications are

Table 1 The list of El Niño years, La Niña years and neutral years during P2 (1998–2010) and P3 (2011–2020)

	P2(1998–2010)	P3(2011–2020)
El Niño years	2002 2004 2006 2009	2014 2015 2018
La Niña years	1998 1999 2000 2007 2010	2011 2016 2017 2020
Neutral years	2001 2003 2005 2008	2012 2013 2019

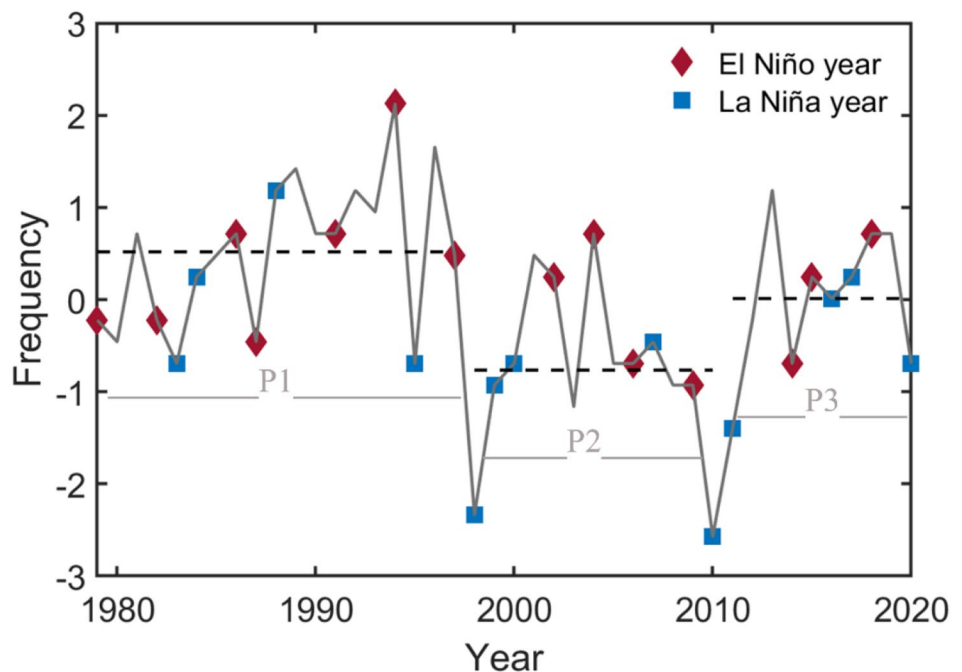shown in Table 1. P1, P2 and P3 represent the periods of 1979–1997, 1998–2010 and 2011–2020, respectively.

2.4 Genesis potential index

To determine the factors that influence changes in TC genesis, we used a modified version of genesis potential index (GPI) (Murakami et al. 2011):

$$GPI = \left|10^5\eta\right|^{3/2}\left(\frac{RH}{50}\right)^3\left(\frac{V_{\text{pot}}}{70}\right)^3(1+0.1V_s)^{-2}\left(\frac{-\omega+0.1}{0.1}\right) \quad (1)$$

where η is the absolute vorticity (s^{-1}) at 850 hPa, RH is the relative humidity (%) at 600 hPa, V_s is the magnitude of the vertical wind shear (ms^{-1}) between 850 and 200 hPa, and ω is the vertical pressure wind velocity (Pa s^{-1}) at 500 hPa, V_{pot} is the maximum potential intensity (PI) (ms^{-1}): $V_{pot}^2 = \frac{C_k T_s}{C_D T_0}(CAPE^* - CAPE^b)$(A MATLAB source code for V_{pot} is available online at http://texmex.mit.edu/pub/emanuel/TCMAX/pcmin.m), C_k is the exchange coefficient for enthalpy, T_s is SST (K), C_D is the drag coefficient, T_0 is the mean outflow temperature (K), $CAPE^*$ is the value of convective available potential energy of the air lifted from saturation at sea level, and the variable $CAPE^b$ is the boundary layer air. To assess the individual importance of these five variables, we recalculate the GPI using the long-term climatology of four variables but varying the annual values for one variable. We carried out this procedure for each of the five variables, followed by recalculating GPI differences between P2 and P3.

2.5 Effective degrees of freedom

In order to consider the reduction in the degrees of freedom of the filtered time series, the effective degrees of freedom, which was used by Chen et al. (2013) and Li and Zhou (2014), are used to evaluate the significance between the filtered variables. The effective degrees of freedom are obtained as n/T, where n is the sample size and $T = \sum_{t=0}^{K} c_{xx}(t) c_{yy}(t)$. c_{xx} and c_{yy} are the autocorrelation coefficients of the two variables with a time lag of t, the maximum of integer K corresponds to $n/2$.

3 TC frequency changes

The present work focuses on the total number of WNP TCs each year (from January to December), and all analyses use the annual mean data. The time series of the WNP TC number is displayed in Fig. 1. Based on the variations, we divide 1979–2020 into three epochs, with turning points in 1998 and 2010, respectively. The number of TCs in the WNP during these two years of turning points is the least. Moreover, 1998 is approximately the PDO phase transition year from the positive to negative (warm to cold) phase (Zhao and Wang, 2016). Compared with P2, there is a significant and abrupt increase in the WNP TC frequency during P3 (Fig. 1). Since the TC frequency between P1 and P2 has been previously studied (e.g., Zhao and Wang, 2016, 2019; Choi and Kim, 2019; Zhao et al., 2021), this study explores

Fig. 1 Time series of standardized TC frequency in the WNP. El Niño years and La Niña years are represented by the red diamond box and blue square box, respectively. The black dashed lines represent the average standardized frequency of TCs in P1 (1979–1997), P2 (1998–2010) and P3 (2011–2020), respectively. The sample standard deviation is calculated over 1979–2020

the reasons for the WNP TC frequency rise during P3 compared to P2.

Figure 2 shows that more TCs can be found during P3 than during P2. The difference between P2 and P3 is 3.3, which is significant at the 95% confidence level. It is shown that the major difference between P2 and P3 is due to the differences during neutral and La Niña years. In La Niña years, the average TC number in P2 (P3) is about 20 (24).

In neutral years, the average TC counts in P2 (P3) are about 23.5 (28.3). In El Niño years, 25.25 (26.33) TCs are observed during P2 (P3). The TC frequency difference in El Niño years, La Niña years and neutral years is significant lower than the 95% confidence level. Figure 2 also shows that there is more TC generation in La Niña years and neutral years during P3 compared to P2. Furthermore, most TCs form in neutral years than in La Niña and El Niño
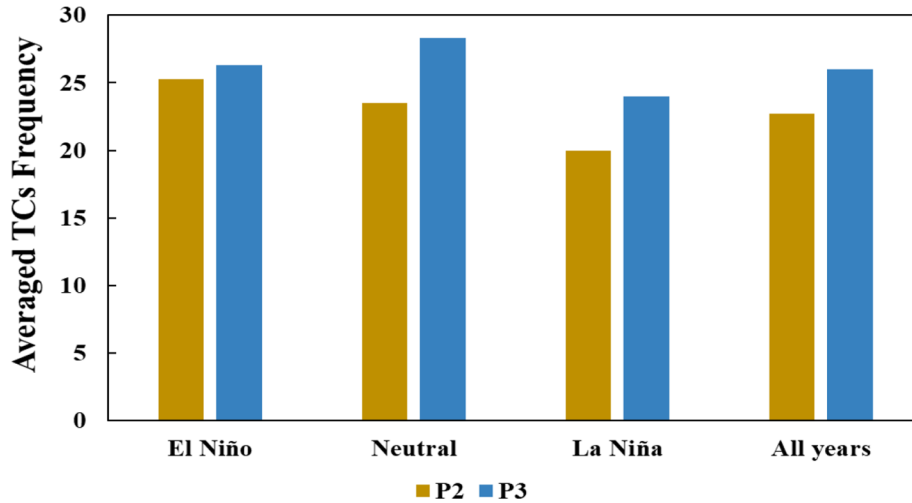
Fig. 2 Mean TC number during El Niño years, neutral years, La Niña years and all years for P2 (1998–2010) and P3 (2011–2020). The TC frequency differences between P2 and P3 are statistically significant at the 95% confidence level for all years, but not for La Niña years, neutral years, and El Niño years. During P2 and P3, the frequency difference between El Niño years and La Niña years is statistically lower than the 95% confidence level
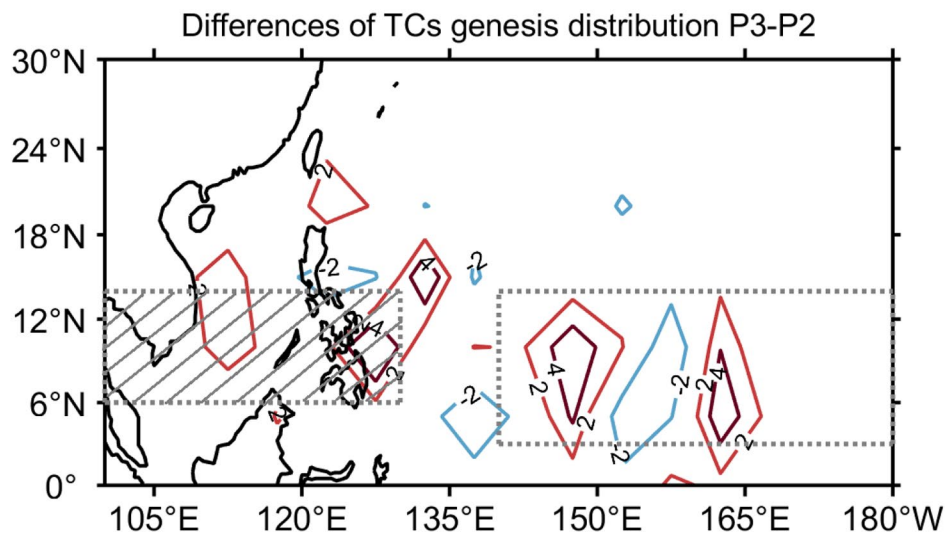
Fig. 3 Differences in WNP TC genesis distribution (×10) between P2 and P3 (P3 minus P2) in each 5° x 5° grid box. The dashed rectangle indicates the region used for TC numbers difference amalgamating in the west (6°-14°N,100°-130°E) and east (3°-14°N,140°E-180°) regions. The slash in the west box indicates significance at the 95% confidence level. The significance in the east box is lower than the 95% confidence level

years in P3, while most TCs are in El Niño years during P2. It is shown that there is no significant change of the TC frequency between P2 and P3 in El Niño years. During P2 and P3, the frequency difference between El Niño years and La Niña years is statistically significant lower than the 95% confidence level.

Figure 3 shows that TCs in the northwest, southeast, and central areas increase significantly during P3 compared to P2. There is a slight reduction in the areas 6°-12°N and 137°-143°E, 12°-18°N and 122°-128°E. The TCs move while they develop, and stochastic factors will also be an issue for TCs. Physical forcing in one region may lead to TC changes in a different region. So here we try to amalgamate TC numbers and average quantities over large regions. The amalgamating TC number difference in the west (6°-14°N,100°-130°E) and east (3°-14°N,140°E-180°) regions is shown in Fig. 3. The TC frequency in the west box increases (1.63) significantly (at the 95% confidence level). However, the TC frequency change in the east box (1.86) is lower than the 95% significant confidence level. TC frequency change is more significant in the western WNP than in the eastern part. More TCs can be observed over the South China Sea

during P3. The genesis of TCs is generally influenced by favorable environmental conditions, such as the increase of the relative vorticity and the decrease of the vertical wind shear, high SST and strengthened vertical velocity (omega). The increase in the relative vorticity at the 850 hPa level can concentrate more convective heating, which is beneficial to the TC development. The vertical wind shear is usually calculated as the difference between wind vectors at 200 hPa and 850 hPa. The decreased vertical wind shear can reduce the advection of heat and moisture from the TC center.

4 Large-scale climate patterns related to TC frequency changes

4.1 Differences in GPI between P2 and P3

Figure 4a shows that GPI differences between P2 and P3 are broadly consistent with the corresponding TC genesis differences over the South China Sea (Fig. 3). There are significant positive areas over the South China Sea. However, some differences also exist in Figs. 3 and 4a, particularly

Fig. 4 Spatial patterns of the genesis potential index (GPI) difference between P2 and P3 (P3 minus P2). (a) GPI; GPI change by (b) vertical wind shear, (c) maximum potential intensity (PI), (d) absolute vorticity, (e) relative humidity, and (f) vertical pressure velocity. Black crosses denote differences that are significant at the 95% confidence level. The dashed rectangle indicates the TC frequency change region of Fig. 3
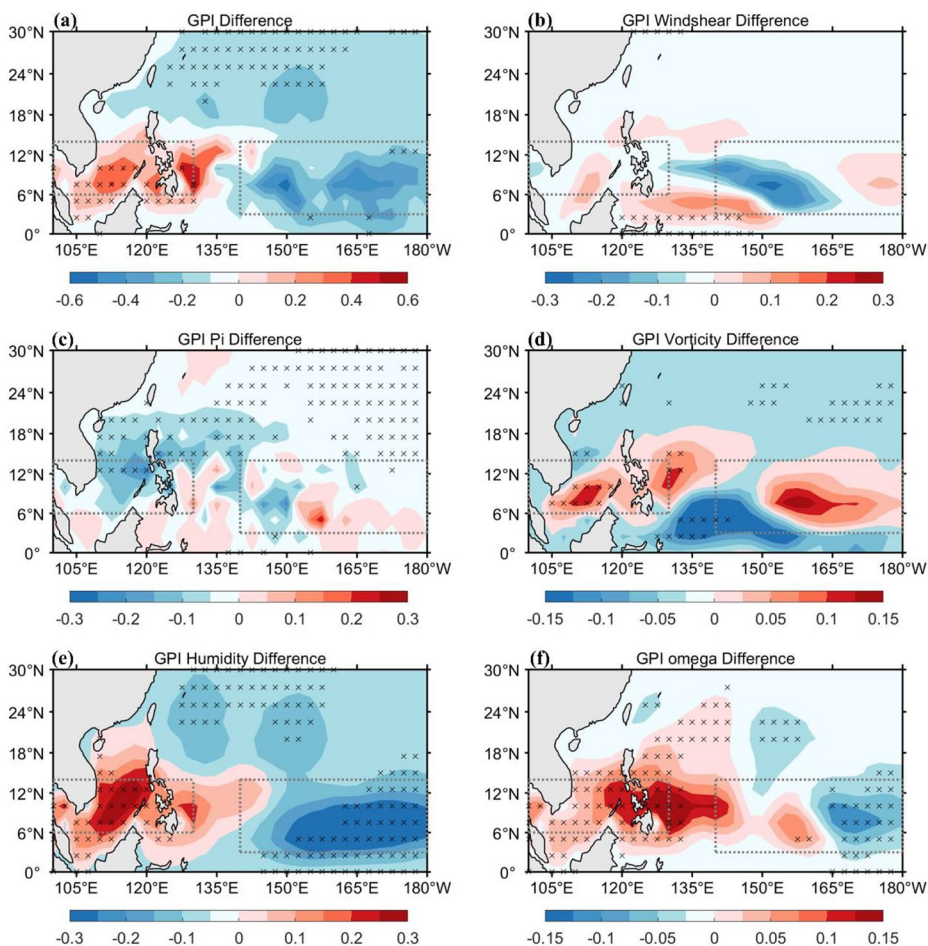
in the eastern box. According to the contribution of the five variables to the GPI in the eastern region, wind shear, relative humidity and PI contribute negatively to the GPI, while relative vorticity and vertical pressure velocity contribute positively to the GPI. The other three terms occupy a large proportion of the equation for calculating GPI, which

Fig. 5 Contributions of each term of Eq. (1) (a) in the whole region: 5°-15°N, 105°E-180°; (b) in the west box: 6°-14°N,100°-130°E; and (c) in the east box: 3°-14°N,140°E-180° of Fig. 3. GPI denotes the GPI change between P2 and P3; Shear denotes the GPI change caused by the vertical wind shear; Vor denotes the GPI change caused by absolute vorticity at 850 hPa; Hum denotes the GPI change caused by the relative humidity at 600 hPa; and W denotes the GPI change caused by the vertical pressure velocity at 500 hPa
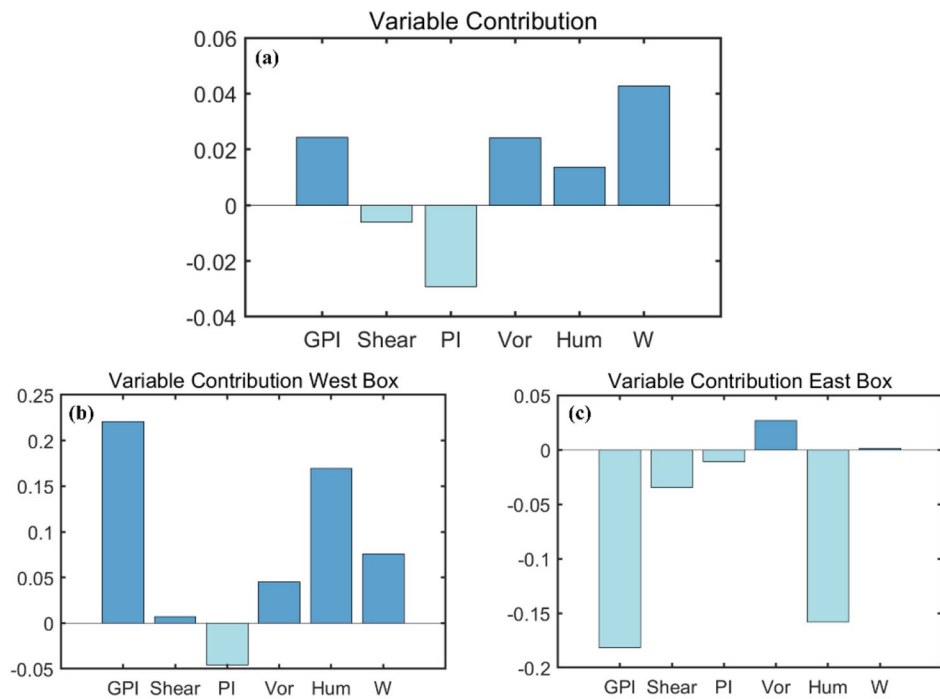
Fig. 6 Contributions of each term of Eq. (1) in the region 5°-15°N, 105°E-180° for each El Niño and La Niña event in P2 and P3. Contribution anomalies for (a)-(e) five La Niña years in P2, (f)-(i) four La Niña years in P3, (j)-(m) four El Niño years in P2, and (n)-(p) three El Niño years in P3, (q) TC frequency anomalies for each El Niño and La Niña years during P2 and P3. Contributions are calculated by allowing one variable to vary while keeping the other variables constant at their climatological values (1998–2020). The anomalies are calculated with the P2 and P3 climatological values (1998–2020)
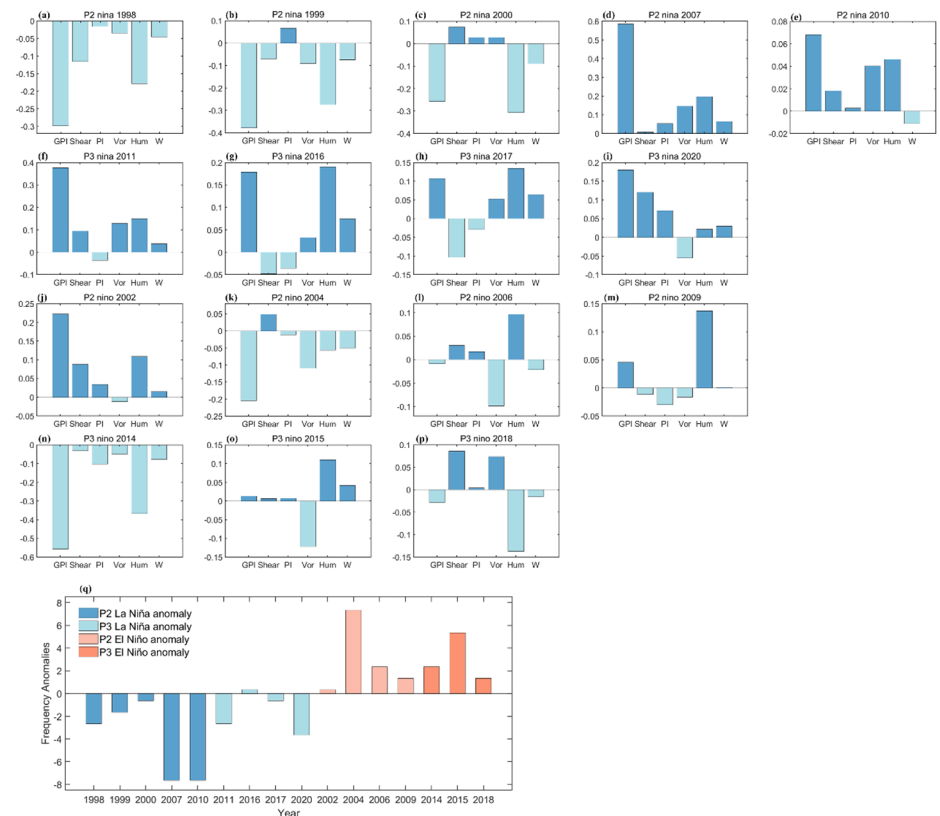
weakens the influence of vertical pressure velocity and relative vorticity. Only small areas of the WNP have significant differences in vertical wind shear (Fig. 4b). Figure 4c shows that the variable PI does not contribute to the TC increase in P3, while the relative vorticity greatly contributes to the increase of TCs frequency in P3 (Fig. 4d). Although the vorticity is not significant in the east of 150°E, the vorticity appears to impact TC formation (Fig. 3). Figure 4e and f indicate that the relative humidity (west box) and vertical pressure velocity are favorable for the TC frequency increase in P3, especially the vertical pressure velocity. These findings suggest that the vorticity, relative humidity and vertical pressure velocity cause more TCs in the western box in P3. Additionally, larger vorticity and vertical pressure velocity play an important role in increasing the TC frequency in the eastern box.

Figure 5 shows the contributions of each term of Eq. (1) to TC genesis. Figure 5a indicates favorable conditions for TC frequency increase in the domain of 5°-15°N, 105°E-180°. The larger vorticity, relative humidity and vertical pressure velocity influence the TC genesis in the domain. The whole GPI is positive, which is in favor of TC genesis. Figure 5b displays the contribution of the five variables to the TC genesis in the west box of Fig. 3. The whole GPI is positive, and wind shear, relative vorticity, relative humidity and vertical pressure velocity contribute positively to TC genesis, except PI. Figure 5c indicates that the whole GPI is negative, the relative vorticity is positive and contribute to the TC genesis. According to the contribution of the five variables to the TC genesis shown in Fig. 5, the relative

vorticity is positive and has an important influence on the TC genesis.

To investigate the differences in environmental variables among El Niño and La Niña events, Fig. 6 displays the anomalies of five environmental variables constituting the GPI, including PI, Hum, Vor, W, and Shear. Figure 6a-e shows the contribution of each term of Eq. (1) in individual La Niña year during P2. In contrast to P2, the GPI in La Niña years of P3 is all positive (Fig. 6f-i), which is favorable for TC genesis. It is consistent with the result shown (Fig. 2) that the TC frequency in La Niña year of P3 is more than that in P2. Figure 6f-i also demonstrates that the vertical pressure velocity at 500 hPa positively contributes to the TC genesis. However, Fig. 6j-p shows that different environmental factors that are beneficial to TC activities in different El Niño year, as previous studies have shown that El Niño does not significantly impact WNP TC number (Li and Zhou, 2013). Figure 6q shows that the TC number generated in La Niña year is less than the number generated in El Niño year in the domain 5°-15°N, 105°E-180°. In La Niña years, the TC number of P3 is greater than that of P2; and in El Niño years, the TC number between P2 and P3 is slightly different.

It is worth noting that the GPI (Fig. 6a-p) has some differences with the TC number. One reason may be that the TC genesis position is not in the selected domain. There are TCs generated outside the selected domain in El Niño or La Niña years. The selected domain has little influence on the generation of these TCs, but has a very important influence on the subsequent development of TCs. Another reason maybe the change of environmental variable that affects

Fig. 7 Differences of (a) relative humidity (%) at 600 hPa, (b) omega (Pa s^{-1}) at 500 hPa, (c) relative vorticity (10^{-6} s^{-1}) at 850 hPa, and (d) vertical wind shear (m s^{-1}) between P2 and P3 (P3 minus P2). The black crosses indicate that the statistical difference in this region is significant at the 95% confidence level
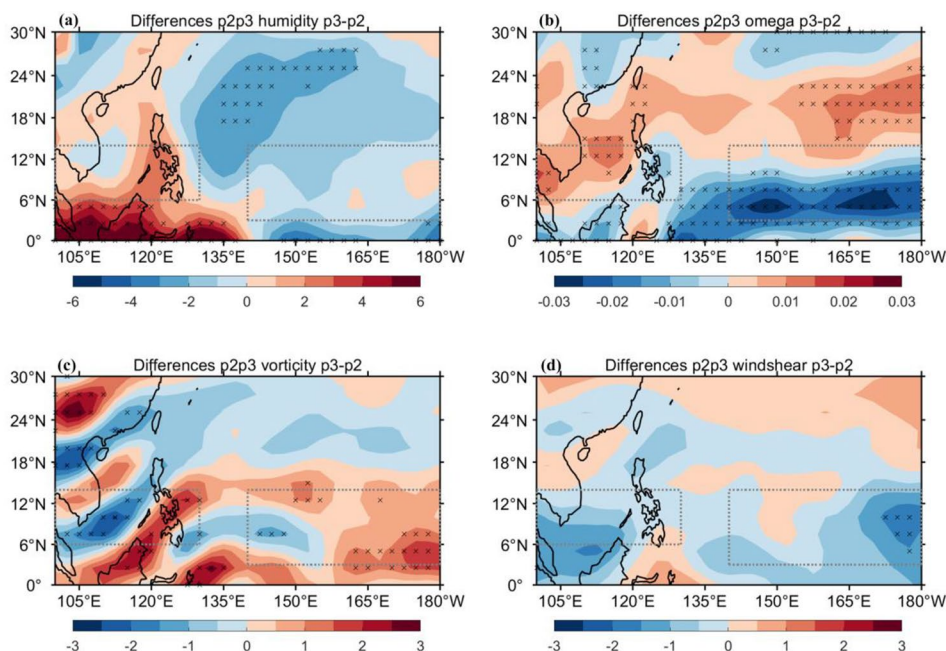
TC activity during El Niño events is complex. Song et al. (2020b) examined the impacts of the three types of El Niño events on TCs over the WNP. They pointed out that different types of El Niño correspond to different environmental factors that are beneficial to TC activities. The TC frequency over western part of the WNP increases when the SST anomalies migrate from east to west. Zhang et al. (2015) reported that the occurrence of TCs in the WNP basin is different during the different kinds of El Niño years.

4.2 Differences in atmospheric conditions between P2 and P3

Figure 7 shows that there are significant positive relative humidity differences in the western box, and a significant enhancement in vertical velocity (omega) in the southeastern part (123°E-180°, 0°-13°N) of the WNP between P2 and P3. An increase in relative vorticity can also be found in 123°E-180°, 0°-18°N area. The increase in TC frequency in the east of the WNP (east of 140°E) is mainly influenced by

Fig. 8 Same as Fig. 7, but for La Niña years
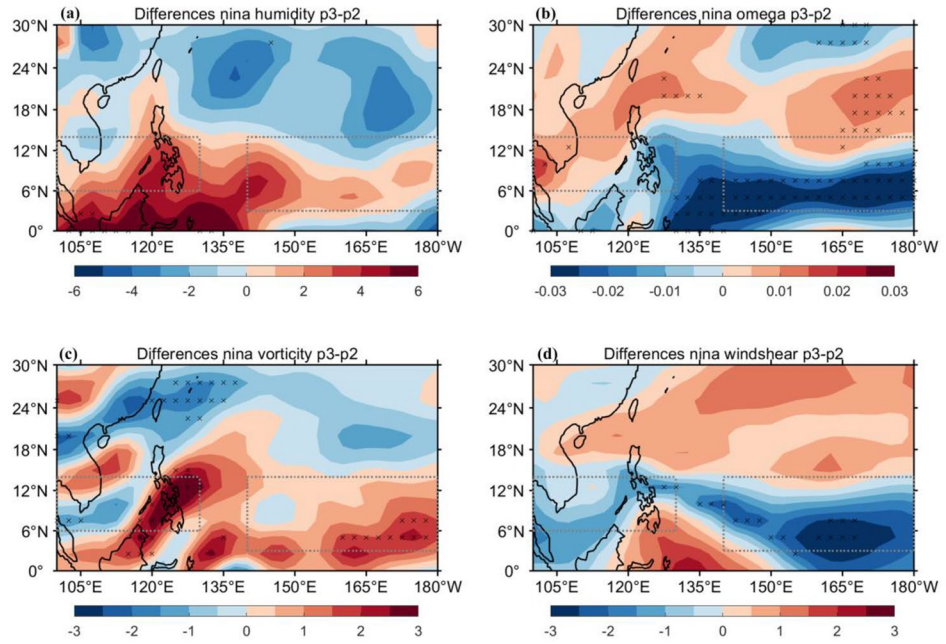


**Fig. 9** Same as Fig. 7, but for El Niño years
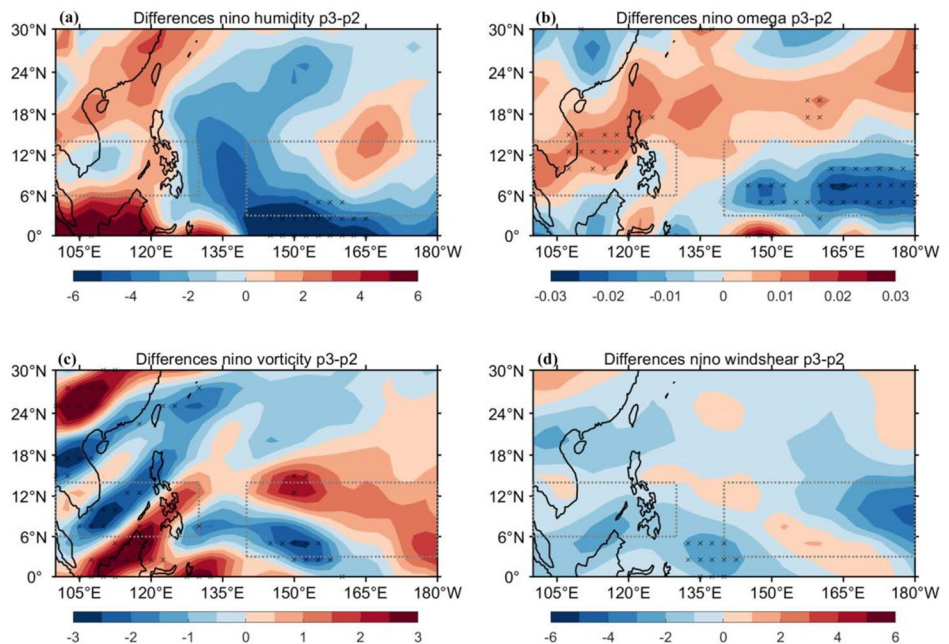
relative vorticity and vertical velocity. Figure 7d also shows that the vertical wind shear in the WNP during P3 is smaller than that during P2. However, only the 165°E-180°,0°-12°N area is significant at the 95% confidence level. We speculate

that conditions in the above areas are conducive to more TC precursor disturbances that can spread to the west or north to develop into TCs in P3 than P2. Corresponding to the genesis position of TCs, we can find that the occurrence of

Fig. 10 SST differences (°C) between (a) P3 and P2, (b) P1 and P2, (c) P3 and P2 in El Niño years, (d) P3 and P2 in La Niña years. The black dots indicate statistical significance at the 95% confidence level
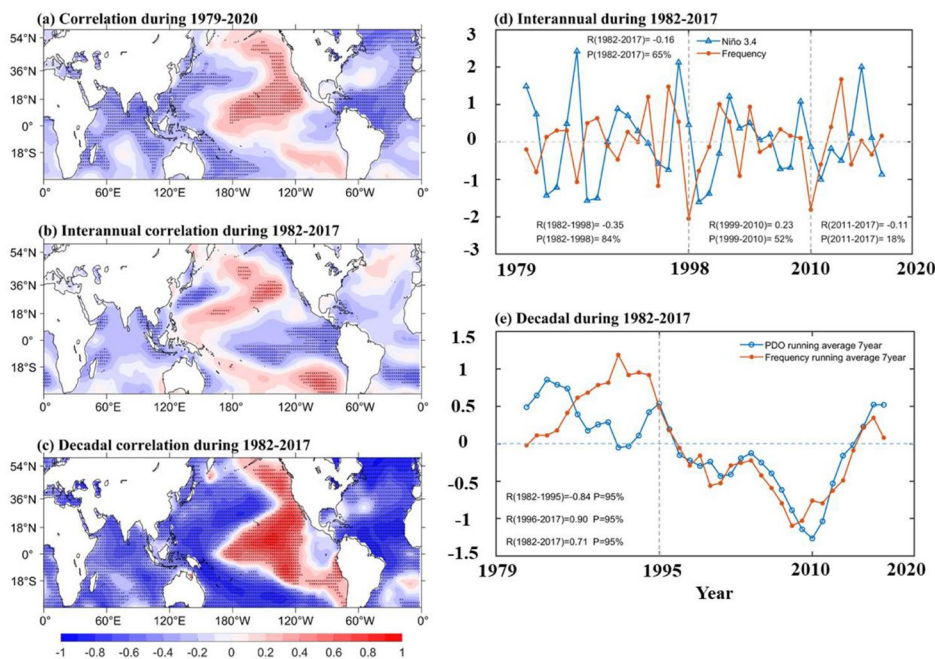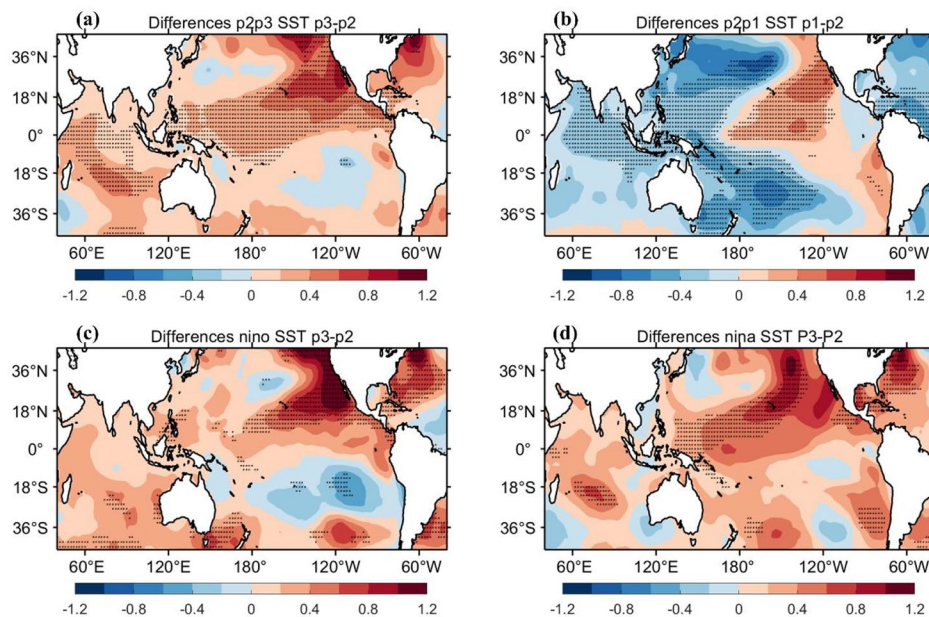
Fig. 11 Correlations between the annual TC frequency and SST (a) during 1979–2020 (all timescales); (b) during 1982–2017 (interannual timescale); (c) during 1982–2017 (decadal timescale). The black dots indicate statistical significance at the 95% confidence level; (d) Time series of the Niño 3.4 index (blue line) and TC frequency (orange line) on interannual timescale, both of which are standardized. (e) Time series of the PDO index (blue line) and TC frequency (orange line). The TC frequency and PDO index are standardized. A 7-year running mean is performed to obtain decadal variability. Interanual variability is calculated by subtracting decadal variability from the total time series

TCs in the western box is mainly affected by relative humidity. The increase in the TC frequency in the eastern box is mainly due to the relative vorticity and vertical velocity. The increase in the TC frequency is mainly related to the relative humidity, the enhanced vertical velocity and the low-level relative vorticity, which is also consistent with the histogram of GPI (Fig. 5).

Figures 8 and 9 display differences in atmospheric conditions between P2 and P3 in La Niña years and El Niño years, respectively. Figure 8 shows that in La Niña years, the vertical velocity (130°E-180°,0°-12°N), the relative vorticity (120°E-180°,0°-18°N), the relative humidity (100°-135°E, 0°-3°N) and the vertical wind shear (135°E-180°,0°-12°N) are conducive to the development of TCs. The large-scale climate differences for El Niño years are shown in Fig. 9. Compared with P2, the favorable factors for the development of TCs in P3 are not significant, although vertical velocity (145°E-180°,2.5°-10°N) and relative vorticity (145°-153°E,12°-15°N; 105°-120°E,0°-8°N) play a role. This also corresponds to the fact that the frequency changes of TCs in El Niño years in Fig. 2 are not significant.

4.3 Relations to SST variations

As suggested by previous studies (Zhan et al., 2011; Hsu et al., 2014; Yamaguchi et al., 2020), the different SST anomaly distributions can impact atmospheric circulation in the WNP. The SST changes in the WNP region are warm between P2 and P3 (Fig. 10), the warm SST anomalies migrate from east to west. We speculate that the higher SST can influence large-scale environmental factors related to TCs. We calculate the correlation of the WNP TC frequency throughout the year (January-December) with SST over the three ocean basins during 1979–2020 (Fig. 11a). A significant negative correlation appears in the northern Indian Ocean, due to the remote SST warming effect on WNP TCs (Wang et al. 2021). The significant negative correlation in the Atlantic Ocean is related to the AMO (Zhang et al. 2018).

Figure 11b shows the interannual relationship between the TCs frequency and SST. The interannual variable is calculated by subtracting the decadal variable which is represented by a 7-year running mean, from the total time series. It shows that a negative relationship appears in the equatorial central and eastern Pacific. The distribution is most likely the ENSO pattern. Figure 11d compares the TC frequency throughout the year (January-December) with the Niño 3.4 index. The correlation during 1982–2017 is -0.16, indicating that ENSO is not significantly correlated with the TC number in the whole WNP (e.g., Wang and Chan 2002). The correlations between the Niño 3.4 index and TC frequency during P1, P2 and P3 are − 0.35, 0.23 and − 0.11,

respectively. Although these correlations are not significant, it is interesting to see the sign change of the correlations. In P1, the correlation is the largest and negative. The larger number of TCs occurs during La Niña events. But during the phase transition of the PDO around 1997, the increase in TC corresponds to the increase in Niño index, and the larger number of TCs appears during El Niño events.

To emphasize the decadal variations, we perform the 7-year running mean on the data and repeat the correlation calculations (Fig. 11c). The patterns of correlation distribution in Fig. 11a are much more similar to Fig. 11c than that to Fig. 11b, indicating that the correlation pattern in Fig. 11a (at both interannual and decadal time scales) is dominated by decadal variability. A significant negative correlation around 36°N can also be seen in Fig. 11a. The correlation patterns in the Pacific are similar to those of the PDO. Therefore, we compare the TC frequency variation at decadal time scales with the PDO index (Fig. 11e). The correlation between the PDO and WNP TC frequency during 1982–2017 is 0.71 which is above the 95% confidence level. Figure 11e also shows that the decadal relationships of WNP TCs with the PDO are opposite before and after the middle 1990s. The correlations during 1982–1995 and 1996–2017 are − 0.84 and 0.90, respectively. The TC frequency is negatively (positively) correlated with PDO index before (after) 1995. The TC frequency in the positive phase of the PDO is larger than that in the negative phase. When the PDO is in the positive phase, the corresponding SST can affect the large-scale environmental factors that are more favorable for TC development.These suggest that in the Pacific, the PDO has a stronger relationship with WNP TCs than ENSO.

4.4 Compared with P1

The TC frequency during the late season (October-December) or from June to August in P1 has previously been studied (Zhao and Wang, 2016, 2019). In this section, the changes in the factors influencing the TC frequency between P1 and P3 are discussed.

Zhao and Wang (2016, 2019) previously point out that the warm phase (P1) is related to the increase in the TC frequency and the decrease of interannual correlation between ENSO and TCs, while the cold phase (P2) is related to the decrease in the TC frequency and the increase in interannual correlation between ENSO and TCs. The changes of relative vorticity and vertical wind shear in the WNP play a major role in the change of the TC frequency during P1 compared to P2. The change in SST in the tropical Indo-Pacific is closely associated with the correlation between ENSO and TCs. According to the analysis of the P3 period, we find that the WNP TC frequency also increases, which are consistent with the result of P1 (Zhao and Wang, 2016,

2019): the PDO influences the WNP TC frequency. The TC frequency is the highest in neutral years and the smallest in La Niña years (Fig. 2), which is different from P1 described in Zhao and Wang (2016): La Niña years are with the highest TC frequency and El Niño years are with the lowest. The TC frequency in El Niño years is no longer the least during P3. This may be caused by the PDO: the correlation between the TC frequency per year and PDO is different during P1 and P3 (Fig. 11e). In addition, the difference between P1 and P3 may be caused by the warmer SST (Fig. 10). The SST gradient between the northern Indian Ocean and WNP influences the South China Sea TC frequency (Li and Zhou, 2014). The WNP SST during the P3 period is higher than that during P2, which is different from P1. Warm SST anomalies in the WNP are observed during P3, which can induce equatorial wind anomalies and thereby further change atmospheric circulations. During the La Niña years of P3, the WNP TC frequency is mainly affected by relative humidity and relative vorticity, as well as by vertical velocity (Figs. 8 and 9).

5 Discussion and conclusions

In this study, the increase in the WNP TC frequency during 2011–2020 is analyzed based on large-scale atmospheric and ocean conditions. During 2011–2020, approximately 26 TCs occurred on average every year in the WNP and caused catastrophic damages to the Philippines and other Asian countries (Fig. 3). In recent years, several studies found a decrease in TC counts during 1979–2010 (Hsu et al., 2014; Zhao and Wang, 2016, 2019). It is associated with ENSO and PDO changes. Previous studies mainly focused on the TC frequency before 2015 and did not investigate the change of the whole year TC frequency after 2015. Investigations of the whole year TC frequency are necessary and useful to improve our understanding of TC activity in the WNP.

Based on the JTWC best-track data, this study examines the variations in the WNP TC frequency between January and December of 1979–2020. The WNP TC count shows a significant decline in 1998 and a rise since 2010, resulting in a low cycle (P2: 1998–2010) and two high cycles (P1: 1979–1997 and P3: 2011–2020). Previous studies have analyzed the decrease between P1 and P2. In this study, the analysis is mainly focused on the increased counts of WNP TCs in P3. A difference in the TC number between P2 and P3 can be found (Figs. 1 and 2). Figure 2 shows that the all year difference between P2 and P3 is significant at the 95% confidence level; however the differences in La Niña years, El Niño years and neutral years are lower than the 95% level. P3 is different from P1 described in Zhao and Wang (2016) where La Niña years are the highest and El Niño

years are the lowest. The reason may be that the larger value of the TC frequency appears in the negative phase of ENSO in P1, while the larger value of the TC frequency appears in the positive phase of ENSO in P3 (Figs. 6q and 11d). It also may be due to the warm SST during the P3 period compared with P2 period (Fig. 10). Li and Zhou (2014) point out that the zonal SST gradient between the cooling WNP SST and the warming northern Indian Ocean SST is not favorable for TC genesis. The warming WNP SST during P3 reduces the zonal SST gradient, resulting in a favorable environment for TC genesis (Liu and Chan, 2020).

Our research also suggests that the changes of dynamical factors like low-level relative vorticity, relative humidity and vertical velocity play an essential role in TC genesis during P3. Vertical velocity, relative vorticity and relative humidity play a major role in La Niña years. For El Niño years, compared with P2, the favorable factors for the development of TCs in P3 are not significant. This also corresponds to the fact that the frequency changes of TCs in El Niño years in Fig. 2 are not significant. The WNP SST has an important influence on TC activity (Hsu et al. 2014; Song et al. 2020). The SST changes in the WNP are characterized by positive SST anomalies in P3 that migrate westward in the North Pacific. We study the correlation between the WNP TC frequency and SST. The result shows that the WNP TC frequency and SST have a significant positive correlation region and a significant negative correlation region. The correlation distributions in the WNP are related to the PDO pattern at decadal time scales (Fig. 11). To further confirm the influence of the PDO, we compare the time series of the PDO and TC frequency. The calculation indicates that the PDO is positively correlated to the frequency of TC. The correlation coefficient is 0.71, which is significant at the 95% confidence level.

SST in P3 is warmer than that in P2, and the positive SST differences are moving towards the western Pacific. This may be one of the reasons why the average TC frequency increases in P3. Warm SST anomalies during the warm phase of the PDO may cause atmospheric circulation anomalies in the WNP which in turn affect TC activity. During the period 2011–2020, the PDO and the warm tropical Pacific SST anomalies are favorable for increasing the TC frequency in the WNP. The large-scale atmospheric environmental conditions like relative vorticity, relative humidity and vertical velocity play a significant role in TC genesis during P3.

References

Bister M, Emanuel KA (1997) The genesis of Hurricane Guillermo: TEX-MEX analyses and a modeling study. Mon Weather Rev 125:2662–2682. https://doi.org/10.1175/1520-0493(1997)1252.0.CO;2

Chen JM, Chen HS, Liu JS (2013) Coherent interdecadal variability of tropical cyclone rainfall and seasonal rainfall in taiwan during october. J Clim 26:308–321. https://doi.org/10.1175/JCLI-D-11-00697.1

Choi JW, Kim HD (2019) Negative relationship between Korea landfalling tropical cyclone activity and Pacific Decadal Oscillation. Dyn Atmos Ocean 87:101100. https://doi.org/10.1016/j.dynatmoce.2019.101100

Choi Y, Ha KJ, Ho CH, Chung CE (2015) Interdecadal change in typhoon genesis condition over the western North Pacific. Clim Dyn 45:3243–3255. https://doi.org/10.1007/s00382-015-2536-y

He H, Yang J, Gong D et al (2015) Decadal changes in tropical cyclone activity over the western North Pacific in the late 1990s. Clim Dyn 45:3317–3329. https://doi.org/10.1007/s00382-015-2541-1

Hsu PC, Chu PS, Murakami H, Zhao X (2014) An abrupt decrease in the late-season typhoon activity over the Western North Pacific. J Clim 27:4296–4312. https://doi.org/10.1175/JCLI-D-13-00417.1

Huang B, Thorne PW, Banzon VF et al (2017) Extended reconstructed sea surface temperature, Version 5 (ERSSTv5): Upgrades, validations, and intercomparisons. J Clim 30:8179–8205. https://doi.org/10.1175/JCLI-D-16-0836.1

Kalnay E, Kanamitsu M, Kistler R, et al (1996) The NCEP/NCAR 40-Year Reanalysis Project. Bull Am Meteorol Soc 77:437–471. https://doi.org/10.1175/1520-0477(1996)0772.0.CO;2

Kim HK, Seo KH, Yeh SW et al (2020) Asymmetric impact of Central Pacific ENSO on the reduction of tropical cyclone genesis frequency over the western North Pacific since the late 1990s. Clim Dyn 54:661–673. https://doi.org/10.1007/s00382-019-05020-8

Kim HM, Webster PJ, Curry JA (2011) Modulation of North Pacific tropical cyclone activity by three phases of ENSO. J Clim 24:1839–1849. https://doi.org/10.1175/2010JCLI3939.1

Kim JH, Ho CH, Kim HS et al (2008) Systematic variation of summertime tropical cyclone activity in the western North Pacific in relation to the Madden-Julian oscillation. J Clim 21:1171–1191. https://doi.org/10.1175/2007JCLI1493.1

Knutson TR, McBride JL, Chan J et al (2010) Tropical cyclones and climate change. Nat Geosci 3:157–163. https://doi.org/10.1038/ngeo779

Li RCY, Zhou W (2013) Modulation of western North Pacific tropical cyclone activity by the ISO. Part I: Genesis and intensity. J Clim 26:2904–2918. https://doi.org/10.1175/JCLI-D-12-00210.1

Li RCY, Zhou W (2014) Interdecadal change in South China Sea tropical cyclone frequency in association with zonal sea surface temperature gradient. J Clim 27:5468–5480. https://doi.org/10.1175/JCLI-D-13-00744.1

Lin II, Chan JCL (2015) Recent decrease in typhoon destructive potential and global warming implications. Nat Commun 6. https://doi.org/10.1038/ncomms8182

Liu C, Zhang W, Geng X et al (2019) Modulation of tropical cyclones in the southeastern part of western North Pacific by tropical Pacific decadal variability. Clim Dyn 53:4475–4488. https://doi.org/10.1007/s00382-019-04799-w

Liu KS, Chan JCL (2020) Recent increase in extreme intensity of tropical cyclones making landfall in South China. Clim Dyn 55:1059–1074. https://doi.org/10.1007/s00382-020-05311-5

Liu KS, Chan JCL, Kubota H (2021) Meridional oscillation of tropical cyclone activity in the western North Pacific during the past 110 years. Clim Change 164. https://doi.org/10.1007/s10584-021-02983-8

Mei W, Xie SP (2016) Intensification of landfalling typhoons over the northwest Pacific since the late 1970s. Nat Geosci 9:753–757. https://doi.org/10.1038/ngeo2792

Mendelsohn R, Emanuel K, Chonabayashi S, Bakkensen L (2012) The impact of climate change on global tropical cyclone damage. Nat Clim Chang 2:205–209. https://doi.org/10.1038/nclimate1357

Molinari J, Vollaro D, Skubis S, Dickinson M (2000) Origins and mechanisms of eastern Pacific tropical cyclogenesis: A case study. Mon Weather Rev 128:125–139. https://doi.org/10.1175/1520-0493(2000)1282.0.CO;2

Murakami H, Wang B, Kitoh A (2011) Future change of western North Pacific typhoons: Projections by a 20-km-mesh global atmospheric model. J Clim 24:1154–1169

Nolan DS, Rappin ED, Emanuel KA (2007) Tropical cyclogenesis sensitivity to environmental parameters in radiative-convective equilibrium. Q J R Meteorol Soc 133:2085–2107. https://doi.org/10.1002/qj.170

Peduzzi P, Chatenoux B, Dao H et al (2012) Global trends in tropical cyclone risk. Nat Clim Chang 2:289–294. https://doi.org/10.1038/nclimate1410

Rayner NA, Parker DE, Horton EB et al (2003) Global analyses of sea surface temperature, sea ice, and night marine air temperature since the late nineteenth century. J Geophys Res Atmos 108. https://doi.org/10.1029/2002jd002670

Ritchie EA, Holland GJ (1997) Scale interactions during the formation of typhoon irving. Mon Weather Rev 125:1377–1396. https://doi.org/10.1175/1520-0493(1997)1252.0.CO;2

Song J, Duan Y, Klotzbach PJ (2020) Increasing trend in rapid intensification magnitude of tropical cyclones over the western North Pacific. Environ Res Lett 15. https://doi.org/10.1088/1748-9326/ab9140

Song J, Duan Y, Klotzbach PJ (2020b) Differences in western North Pacific tropical cyclone activity among three El Niño phases. J Clim 33:7983–8002. https://doi.org/10.1175/JCLI-D-20-0162.1

Timmermann A, An S, Il, Kug JS et al (2018) El Niño–Southern Oscillation complexity. Nature 559:535–545. https://doi.org/10.1038/s41586-018-0252-6

Trenberth KE, Caron JM (2000) The southern oscillation revisited: Sea level pressures, surface temperatures, and precipitation. J Clim 13:4358–4365. https://doi.org/10.1175/1520-0442(2000)0132.0.CO;2

Tu JY, Chou C, Chu PS (2009) The abrupt shift of typhoon activity in the vicinity of Taiwan and its association with western North Pacific-East Asian climate change. J Clim 22:3617–3628. https://doi.org/10.1175/2009JCLI2411.1

Vecchi GA, Soden BJ (2007) Effect of remote sea surface temperature change on tropical cyclone potential intensity. Nature 450:1066–1070. https://doi.org/10.1038/nature06423

Vu T, Kieu C, Chavas D, Wang Q (2020) A numerical study of the global formation of tropical cyclones. J Adv Model Earth Syst 1–33. https://doi.org/10.1029/2020ms002207

Walsh KJE, Sharmila S, Thatcher M et al (2020) Real world and tropical cyclone world. Part II: Sensitivity of tropical cyclone formation to uniform and meridionally varying sea surface temperatures under aquaplanet conditions. J Clim 33:1473–1486. https://doi.org/10.1175/JCLI-D-19-0079.1

Wang B, Chan JCL (2002) How strong ENSO events affect tropical storm activity over the western North Pacific. J Clim 15:1643–1658. https://doi.org/10.1175/1520-0442(2002)0152.0.CO;2

Wang C, Wu K, Wu L et al (2021) What caused the unprecedented absence of western North Pacific tropical cyclones in July 2020? Geophys Res Lett 48:1–9. https://doi.org/10.1029/2020GL092282

Wang Q, Li J, Li Y et al (2018) Modulation of tropical cyclogenesis location and frequency over the Indo-western North Pacific by the intraseasonal Indo-western Pacific convection oscillation during the boreal extended summer. J Clim 31:1435–1450. https://doi.org/10.1175/JCLI-D-17-0085.1

Wang X, Wang C, Zhang L, Wang X (2015) Multidecadal variability of tropical cyclone rapid intensification in the western North Pacific. J Clim 28:3806–3820. https://doi.org/10.1175/JCLI-D-14-00400.1

Yamaguchi M, Chan JCL, Moon IJ et al (2020) Global warming changes tropical cyclone translation speed. Nat Commun 11:1–7. https://doi.org/10.1038/s41467-019-13902-y

Yang L, Chen S, Wang C et al (2018) Potential impact of the Pacific Decadal Oscillation and sea surface temperature in the tropical Indian Ocean–Western Pacific on the variability of typhoon landfall on the China coast. Clim Dyn 51:2695–2705. https://doi.org/10.1007/s00382-017-4037-7

Yokoi S, Takayabu YN (2013) Attribution of decadal variability in tropical cyclone passage frequency over the western North Pacific: A new approach emphasizing the genesis location of cyclones. J Clim 26:973–987. https://doi.org/10.1175/JCLI-D-12-00060.1

Zhan R, Wang Y, Wu CC (2011) Impact of SSTA in the east Indian Ocean on the frequency of northwest Pacific tropical cyclones: A regional atmospheric model study. J Clim 24:6227–6242. https://doi.org/10.1175/JCLI-D-10-05014.1

Zhan R, Wang Y, Ying M (2012) Seasonal forecasts of tropical cyclone activity over the western North Pacific: A Review. Trop Cyclone Res Rev 1:307–324. https://doi.org/10.6057/2012TCRR03.07

Zhang G, Zeng G, Li C, Yang X (2020) Impact of PDO and AMO on interdecadal variability in extreme high temperatures in North China over the most recent 40-year period. Clim Dyn 54:3003–3020. https://doi.org/10.1007/s00382-020-05155-z

Zhang Q, Wu L, Liu Q (2009) Tropical cyclone damages in China 1983–2006. Bull Am Meteorol Soc 90:489–495. https://doi.org/10.1175/2008BAMS2631.1

Zhang W, Leung Y, Fraedrich K (2015) Different El Niño types and intense typhoons in the Western North Pacific. Clim Dyn 44:2965–2977. https://doi.org/10.1007/s00382-014-2446-4

Zhang W, Vecchi GA, Murakami H et al (2018) Dominant role of Atlantic Multidecadal Oscillation in the recent decadal changes in western North Pacific tropical cyclone activity. Geophys Res Lett 45:354–362. https://doi.org/10.1002/2017GL076397

Zhang W, Vecchi GA, Villarini G et al (2017) Modulation of western North Pacific tropical cyclone activity by the Atlantic Meridional Mode. Clim Dyn 48:631–647. https://doi.org/10.1007/s00382-016-3099-2

Zhang X, Zhong S, Wu Z, Li Y (2018b) Seasonal prediction of the typhoon genesis frequency over the western North Pacific with a Poisson regression model. Clim Dyn 51:4585–4600. https://doi.org/10.1007/s00382-017-3654-5

Zhao H, Wang C (2016) Interdecadal modulation on the relationship between ENSO and typhoon activity during the late season in the western North Pacific. Clim Dyn 47:315–328. https://doi.org/10.1007/s00382-015-2837-1

Zhao H, Wang C (2019) On the relationship between ENSO and tropical cyclones in the western North Pacific during the boreal summer. Clim Dyn 52:275–288. https://doi.org/10.1007/s00382-018-4136-0

Zhao J, Zhan R, Wang Y, Xu H (2018) Contribution of the interdecadal pacific oscillation to the recent abrupt decrease in tropical cyclone genesis frequency over the western North Pacific since 1998. J Clim 31:8211–8224. https://doi.org/10.1175/JCLI-D-18-0202.1

Zhao K, Zhao H, Raga GB et al (2021) Changes in extended boreal summer tropical cyclogenesis associated with large-scale flow patterns over the western North Pacific in response to the global warming hiatus. Clim Dyn 56:515–535. https://doi.org/10.1007/s00382-020-05486-x